ELSEVIER

Journal of Power Sources 96 (2001) 106–112

JOURNAL OF POWER SOURCES

www.elsevier.com/locate/jpowsour

On the impedance of the gassing reactions in lead-acid batteries

Abderrezak Hammouche*, Eckhard Karden, Jörg Walter, Rik W. De Doncker

Institute for Power Electronics and Electrical Drives, Aachen University of Technology, Jägerstrasse 17-19, D-52066 Aachen, Germany

Received 29 November 2000; accepted 16 December 2000

Abstract

Oxygen and hydrogen evolution reactions in flooded lead-acid batteries during float charging were studied by galvanostatic steady-state polarization and impedance spectroscopy techniques. Given the very low relaxation frequencies of such processes (between 2 and 0.05 mHz), impedance measurements needed to be extended to the ultra-low frequency domain. Investigation of their dynamic behavior provided a complete description of the porous character of the active zone. The steps involved in the reaction mechanisms are also discussed.

Keywords: Lead-acid batteries/flooded; Polarization; Gas evolution reactions

1. Introduction

The purpose of float charging is to maintain a battery in a full state of charge and to return it to that state after it has undergone a discharge. This is accomplished by applying a voltage slightly higher than the open-circuit voltage of the fully-charged battery, to compensate for unavoidable gradual self-discharge.

Lead-acid batteries are especially suited for float charging, because they can be recharged completely at float voltage and retain full capacity when charged continuously at a fairly low float voltage of about 100–150 mV per cell above open-circuit.

In lead-acid batteries, completion of charge is followed by "gassing", that is to say oxygen evolution at the positive plate and that of hydrogen at the negative one

$$2H_2O = O_2 + 4H^+ + 4e^-, \quad E_{H_2O/O_2} = 1270\,\text{mV} \text{ vs. SHE}$$

$$2H^+ + 2e^- = H_2, \quad E_{H_2/H^+} = -365\,\text{mV} \text{ vs. SHE}$$

The generation of such gases can never be completely suppressed because hydrogen evolution starts above the equilibrium potential of the negative ($Pb/PbSO_4$) electrode, and oxygen evolution below the equilibrium potential of the positive ($PbSO_4/PbO_2$) electrode. In order to prevent water loss caused by gassing, many attempts were made either by hindering such processes by the use of lead–calcium and low-antimony grids (which, unfortunately, are not without side effects) or better, by recombining, chemically and/or electrochemically, the hydrogen and oxygen gases given off during overcharging.

Another relevant reaction in such conditions is corrosion of lead in the current-collector, which reduces the lead dioxide, taking place at the rest potential without any outside current.

Knowing the high time constants of the processes occurring in the lead-acid battery (many tens of hours are usually needed to allow the dc signals relax), Karden and coworkers [1,2] developed in the last few years a specialized impedance spectroscope to investigate the dynamic behavior of such systems in the microhertz frequency range, taking into account all the specific requirements of industrial batteries. Applied to a set of 100 Ah lead-acid cells, it showed good reproducibility and consistency of the results.

Because of the limited understanding of gas evolution mechanisms and the resulting uncontrolled life expectancy of lead-acid batteries, further studies are needed. Lead and lead dioxide plates present a rather poor catalytic activity towards, respectively, hydrogen and oxygen evolution [3,4]. It can then be expected that their time constants will be very high. Consequently, the method of ultra-low frequency impedance spectroscopy is especially suitable for investigation of such processes.

The purpose of this study is to analyze the electrochemical processes occurring at both plates in a flooded lead-acid battery when in the overcharge region, by dc polarization and ultra-low frequency impedance spectroscopy.

* Corresponding author. Tel.: +49-241-80-69-45; fax: +49-241-67-505.
E-mail address: hm@isea.rwth-aachen.de (A. Hammouche).

0378-7753/01/$ – see front matter
PII: S0378-7753(01)00488-8

2. Experimental

All experiments were performed with a flooded 4GroE100 cell, made by Hoppecke, with a nominal C_{10} capacity of 100 Ah. The electrolyte was a sulfuric acid solution with a density of 1.22 kg l^{-1}. The temperature of measurements, 23°C, was constant to within 1°C.

Impedance measurements were performed during float operation after charging the cell with a high charge coefficient and after several days of float operation at a fixed voltage of 2.23 V. In fact, this voltage value, which corresponds to the minimum rate of grid corrosion, is usually recommended for float operation. The impedances of the full cell and of both half-cells were successively measured galvanostatically with dc currents ranging from 40 to 270 mA, after stabilization during 30 h for each dc current. Laboratory instrumentation, used for the present experiments, has been developed at ISEA for high-precision impedance measurements of industrial batteries [2].

The ac current amplitude was automatically chosen for each frequency so that the optimum ac voltage response was always equal to 3 mV (which is well below the thermal energy "$RT/F = 25$ mV" at room temperature and more than two orders of magnitude below the dc overvoltages). Also, the upper ac current value was limited to 2/3 of the dc current value, to keep the net current $[I(t) = I_{dc} + I_{ac}\sin(\omega t)]$ always within the charging regime and so prevent occurrence of the battery discharging during the negative half-period of the ac signal.

The frequency range was 3 kHz–38 μHz with eight frequencies per decade for the cell and the positive plate. Each spectrum required a measuring time of almost 4 days (the measurement of Z at 38 μHz alone lasts $3/38 \times 10^6$ s, ≈22 h). Knowing that very slow dynamics exist in the battery, it would be desirable to go even further, but adding one frequency decade makes the measuring time 10 times as long. The time required for a single experiment would then be counted in months rather than days. However, the frequency range for the negative plate was taken down to only 150 μHz as this covered mostly its whole relaxation frequency range, as can be seen on the experimental data. The initial parts of the spectra (down to 1 mHz) were usually repeated after the first spectrum to check if the experimental conditions were stationary. These measurements were always in good agreement with each other.

Unfortunately, our test bench does not yet allow for multichannel voltage measurement. Therefore, we measured the cell impedance and the electrode impedances in subsequent experiments. Anyway, the sum of both half-cell impedances turns out to be always very close to the cell impedance, though all three quantities were measured in different experiments, each of which lasting several days.

The experimental data were fitted to the relevant equations using the least-square fit, built-in with Excel, to optimize the parameters. In the case of impedance diagrams, the real and the imaginary components were fitted at the same time through minimizing the sum of the "weighted" squares of the difference between the measured ($Z_m(\omega)$) and the simulated ($Z_s(\omega)$) data sets

$$S = \sum_{i=1}^{n} w_i[(Z'_m - Z'_s)^2 + (Z''_m - Z''_s)^2]$$

Only one weight factor, w_i, was used as both data sets are not independent of each other. It is equal to the inverse of the square of the modulus of the impedance, $w_i = 1/(Z'_m 2 + Z''_m 2)$, letting each measurement contribute equally to the sum of squares.

We used a mercury/mercurous sulfate reference electrode (RE), of standard design, in the same sulfuric acid concentration as the cell electrolyte, to measure the electrode potentials separately and avoid liquid junction potential error. Its thermodynamic potential, in the 1.22 kg l^{-1} H_2SO_4 solution at 23°C, is estimated to be 606.5 mV versus SHE [5]. The RE tip was located in the midpoint between the two current collecting tabs and 20 mm above the top of the plates.

3. Results and discussion

3.1. Current and potential distribution near the tabs

According to Newman's reports on half-cell investigations on lead-acid batteries [6], RE measurements are most meaningful when the exact position of RE is specified. Actually, distribution of current lines and equipotential surfaces in lead-acid batteries is deeply affected by the limited electrical conductivity of the plate's grid. A non-homogeneous current and potential distribution entails a heterogeneous utilization of the plates and so a loss in capacity.

Orientation of current lines can be inferred from the variations of the ohmic resistance measured between a working and a reference electrode, this latter being located in different positions in the cell. Since, the diameter of the RE used was too large to be inserted into the limited space between the plates, where heterogeneity of current and potential is expected to be more pronounced, impedance measurements were performed in the present study only for positions in the free solution above the plates, near the tabs (Fig. 1).

No significant effect was observed in the impedance of the electrodes whatever the position of RE, but the ohmic resistance between either tab and RE was sensitive when RE was moved horizontally in the x direction (i.e. parallel to the plates), for different values of y and z. As RE came near one tab, the respective ohmic resistance decreased while that corresponding to the opposite tab increased (Fig. 2). The sum of these partial resistances was, however, very close to the one measured for the complete cell.

It can readily be inferred from this observation that the current lines in this region are rather oriented towards the

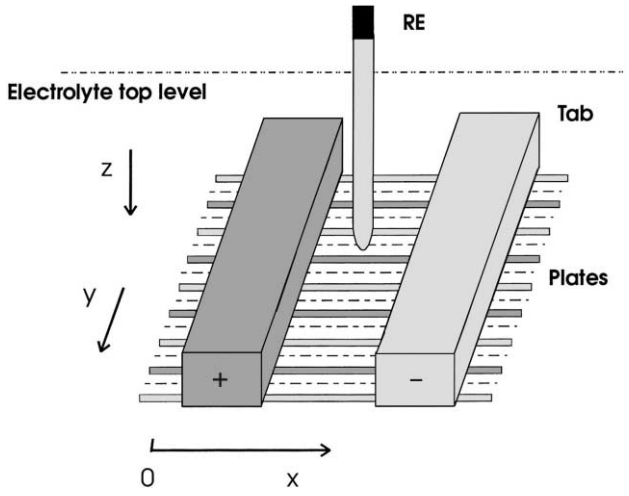

Fig. 1. Location of the reference electrode for half-cell measurements.

tabs, suggesting that these take part to some extent in the electrode processes. This statement is confirmed by observation of some gas bubbles given off from the surface of the tabs, in float charge conditions. Since, gassing reactions give rise to additional water loss, it is desirable to suppress them. This may be achieved, for instance, by covering the tabs with an insulating substance.

In the subsequent measurements, RE was definitely placed in the midpoint between the two current collecting tabs and 20 mm above the top of the plates.

3.2. Polarization curves (dc)

From a fundamental point of view, float charging of a fully-charged battery seems to be the only experimental situation in which the electrochemical processes can be regarded as stationary. The only change in the chemical compositions within the cell is caused by the gassing reactions which consume water, but do not significantly change the electrolyte concentration on time scales out to many days. Besides, the gas bubbles cause some convection which makes it plausible that the electrolyte concentration is almost constant all over the cell.

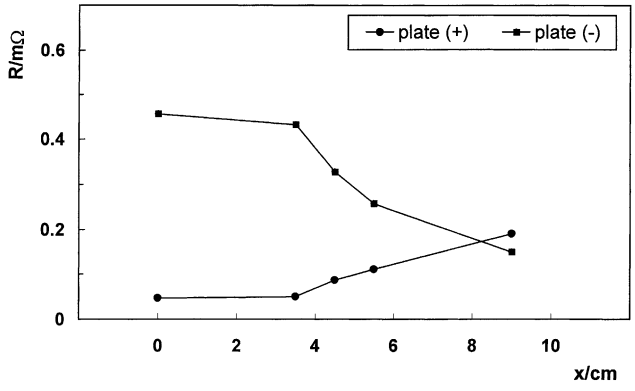

Fig. 2. Variation of ohmic resistance of the half-cells as a function of location of the reference electrode.

Most of the float current flows through the gassing reactions during overcharge, while only a very small fraction of the total current is consumed by the parallel side reactions. It is, thus, expected that both the dc current/voltage and the impedance characteristics of the electrodes are essentially determined by the gassing reactions.

At open circuit and on overcharge in the lead-acid battery, the overvoltages for oxygen and hydrogen evolution are large ($\eta_{O_2} > +434\,\text{mV}$ and $\eta_{H_2} < -359\,\text{mV}$). If these electrochemical processes are under activation control, their kinetics exhibits a Tafel behavior, i.e. a linear potential–log current relationship of the form

$$\eta = U_T \log\left(\frac{I}{I_0}\right) \tag{1}$$

where $\eta = U - U_0$, the overpotential of each reaction; and I_0, the exchange current which is a parameter depending on the concentration of reacting species. The temperature and the transfer coefficient α, give $U_T = 2.3RT/\alpha nF$ which defines the Tafel slope.

If this law is valid for both half-cell reactions and no parallel reactions occur, a similar law holds for the whole cell voltage

$$\begin{aligned} U &= U_{0(O_2/H_2)} + \eta_{O_2} + \eta_{H_2} \\ &= U_{0(O_2/H_2)} + U_{T,H_2} \log\left(\frac{I_{0,O_2}}{I_{0,H_2}}\right) \\ &\quad + (U_{T,O_2} + U_{T,H_2}) \log\left(\frac{I}{I_{0,O_2}}\right) \\ &= \text{Cste} + U_{T,\text{cell}} \log\left(\frac{I}{I_{0,O_2}}\right) \end{aligned}$$

This equation also shows that the Tafel slope for the complete cell is given by adding up the Tafel slopes of the electrode reactions.

The dc cell and half-cell polarization curves were plotted considering the proper currents involved in the main reactions, obtained by subtracting the currents corresponding to the side reactions. Cathodic currents were corrected for that corresponding to oxygen reduction at the negative plate; its value, independent on overvoltage, was estimated to −2.5 mA [7]. Anodic currents were corrected for that corresponding to grid corrosion, which depends on the positive plate overvoltage, showing its minimum at $\eta \sim +80$ mV [7].

Fig. 3 depicts the Tafel plots for the whole cell and the individual electrodes. These slopes are, respectively, 215.3, 127.8 and 81.4 mV per current decade for the cell, the negative and the positive plates. The Tafel slope for the cell is slightly greater than the sum of the slopes for the electrodes. This is related to the fact that the raw float current used for the calculations concerning the cell, includes the contribution of the secondary reactions. Their

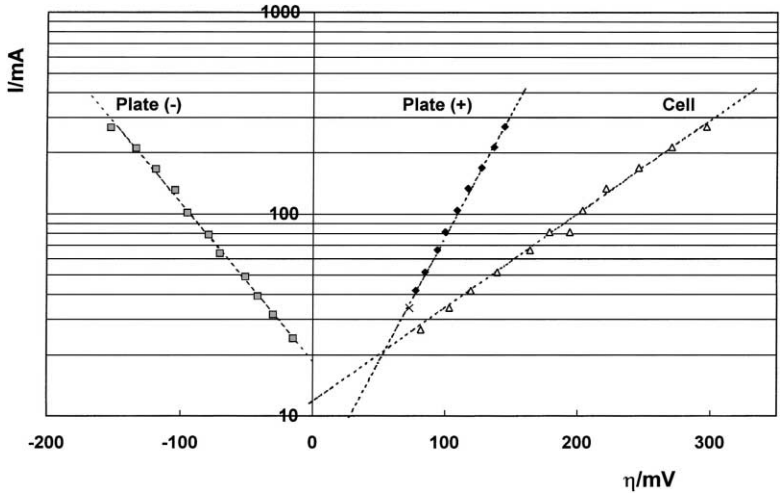

Fig. 3. Float current vs. electrode and cell overvoltages.

effect is somewhat more influential in the low current–overpotential values.

The law, mentioned above, was empirically well defined in a Varta technical report [8]. The overcharging voltage of a lead-acid battery increases by 200 mV per current decade, at room temperature. This increase is shared between the electrode potentials: 120 mV for the negative electrode, and 80 mV for the positive electrode, per current decade. The slight discrepancy shows that these kinetic parameters are dependent on cell design and materials, methods of manufacture and cell age.

3.3. Impedance measurements

3.3.1. Negative plates

A typical impedance diagram under non-zero dc current is shown in Fig. 4. It is mainly composed of a single depressed semicircle. This semicircle can be viewed as approximately equivalent to the response of a simple parallel RC circuit, describing a CPE element. The R_{ct} value measured at the limit of low frequencies corresponds to the slope of the steady-state $I(\eta)$ curve at the corresponding polarization. The agreement between these two values indicates that the recorded diagrams describe the full cell response: there are no other semicircles at lower frequencies.

According to the present results, investigation of the ultra-low frequency domain is necessary since the frequency of the maximum of such semicircles decreases to about 100 μHz, for the low values of float current. This seems to be logical with regards to the poor catalytic activity of lead towards hydrogen evolution, characterized by a very low exchange current density ranging between 10^{-8} A cm^{-2} [3] and 10^{-11} A cm^{-2} [4]. Actually, for batteries with a large electrode surface area, the double-layer electrode

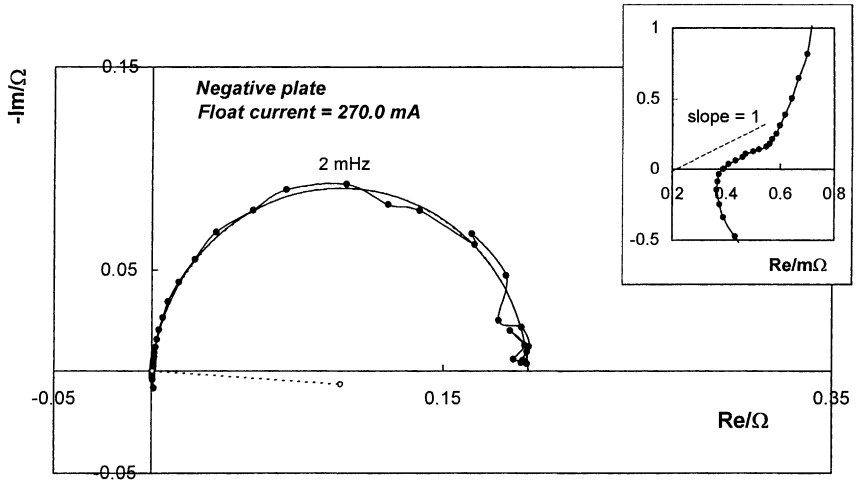

Fig. 4. Typical impedance diagram obtained for the negative plate, under an overcharge current of 270.0 mA. The magnification in the top right part of the figure concerns the high frequency region of the impedance diagram.

capacitance is very large while the charge transfer resistance is not small enough. Consequently, the relaxation frequency, given by the quantity $(2\pi R_{ct}C_{dl})^{-1}$, will go down to the millihertz range. Moreover, if the reaction mechanism involves additional steps like adsorption of electroactive species and/or diffusion processes, the relevant relaxation frequencies will be even lower. Similar experiments reported in the literature were restricted to more than 1 mHz [9], showing only the high frequency branch of the impedance diagram, which appeared more or less vertical. Accordingly, the explanation based on a quasi-blocking character, reported for the electrodes investigated, does not describe actually their electrochemical behavior.

A more careful analysis of the experimental diagrams at high frequencies reveals a straight line in the capacitive quadrant (see the magnified part of the diagram in Fig. 4). Even after correcting for the likely influence of the inductance of the wiring and the intrinsic inductance of the measuring cell (generally ranging between 20 and 200 nH) on the cell impedance in this frequency region [10], the slope of such a line always keeps a value close to unity. This impedance segment is characteristic of the infinite pore behavior of porous electrodes in the high frequency region, where the penetration depth of the alternating signal does not reach the bottom of the pore, when Z identifies to a simple parallel RC circuit [11]. This result indicates that the hydrogen evolution reaction takes place at the internal surface of the electrode pores.

According to the general features of the impedance spectra, the polarization resistance R_{ct} characterizes a charge transfer reaction. This quantity corresponds to the slope, $dU/dI = U_T/I$, of the stationary dc curve $\eta = f(I)$ obtained by differentiating Eq. (1). As can be deduced from the recorded spectra, the variations of R_{ct} with overpotential also obey an exponential law. Accordingly, the product of this resistance times the dc current does not vary with the electrode overpotential. It defines the Tafel slope of the electrode and it is approximately equal to 131.9 mV per decade, showing a good agreement with the data obtained from dc polarization measurements.

The electrode capacitance, estimated as a fitting parameter, has a value decreasing from approximately 70 to 50 F when the electrode potential decreases from −380 to −520 mV versus SHE. This capacitance corresponds to the electrode double layer (C_{dl}). Its large order of magnitude confirms that not only the external surface of the plate is active, but that the internal pore zones are involved in the electrode process as well. Based on a unit surface capacitance of 18 mF cm^{-2}, given in the literature for the lead electrode [12], the mean active surface can be estimated to about 300 m^2, which is consistent with the rough estimation deduced from morphology parameters.

It is worthy of note that the decrease of the electrode capacitance is expected as the potential decreases in the explored range. This fact can be related to the decrease of the specific adsorption of mainly SO_4^{2-} anions as the potential approaches that of zero charge, lying at −620 mV versus SHE for the lead electrode [13].

3.3.2. Positive plates

The general shape of the impedance diagrams obtained for the positive plate is shown in Fig. 5. Two capacitive loops can be distinguished, respectively, around 4 and 0.1 mHz. The order of magnitude of such relaxation frequencies confirms once again the importance of investigating the ultra-low frequency domain. The resistive component associated with both of these loops decreases as the float current increases, but the low frequency loop, being greater, masks completely the higher frequency one under low values of float current.

The mean value of the Tafel slope deduced from these impedance data is 74.3 mV per decade. It represents the sum of 7 and 67.3 mV per decade of Tafel slopes determined for the high and low-frequency loops, respectively. This value is somewhat smaller than the one obtained from the dc polarization data.

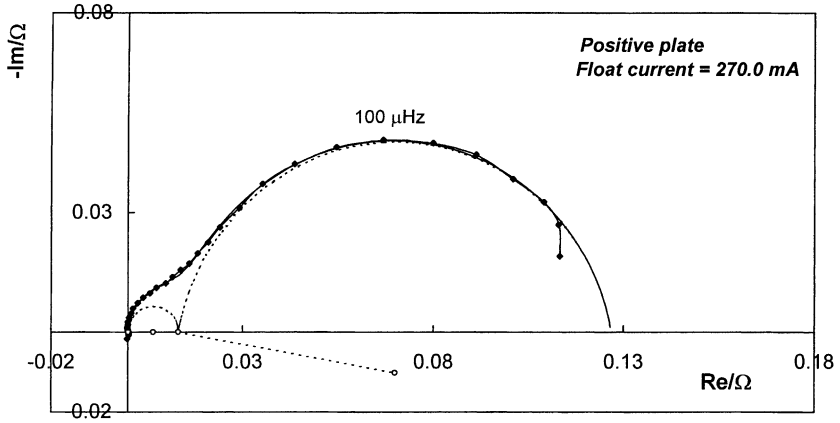

Fig. 5. Typical impedance diagram obtained for the positive plate, under an overcharges current of 270.0 mA.

3.4. Mechanisms of hydrogen and oxygen evolution

3.4.1. Hydrogen electrode reaction

On the most of soft metals in groups 5B and 6B of the periodic table, such as Pb, Bi, Cd, In, Sn and Hg, the hydrogen electrode reaction takes place according to the following two-step mechanism, consisting of a rate determining charge transfer step:

$$H^+ + e^- + s \rightarrow H_{ads}$$

followed by a fast ion–atom recombination

$$H^+ + H_{ads} + e^- = H_2$$

The latter step is in a quasi-equilibrium state. The coverage θ by adsorbed hydrogen atoms must be very low, since none was ever detected, even at the highest overpotentials measured [3]. The rate of the overall reaction is equal to twice that of the first step and is given by

$$I = I_0 \exp\left(\frac{-\alpha nF\eta}{RT}\right) \quad (2)$$

where $I_0 = 2Fk_1(H^+)(1-\theta)\exp(-\alpha nFU_{eq}/RT)$ is the exchange current of the overall reaction, where k_1 is the constant rate of the first step, H^+ the activity of protons, and U_{eq} the equilibrium potential.

Eq. (2) is applicable at high overpotentials, where the reverse reaction can be ignored. Also, it is assumed that mass transport limitation is negligible, which is true in view of the high sulfuric acid concentration. This equation can be written in a logarithmic form as

$$\eta = U_T \log(I) + b$$

where $U_T = 2.3RT/\alpha nF$ and $b = -U_T \log(I_0)$.

The experimental results corresponding to hydrogen evolution on the negative plate fit this equation. The mean Tafel slope of 130 mV per decade corresponds to a transfer coefficient of 0.45, close to the value (0.5) which is characteristic of this family of metals [3]. Moreover, the exchange current density, deduced by extrapolation of the Tafel curve to $\eta_{H_2/H^+} = 0$ mV, and based on the actual surface area ($S_{Pb} = 300\ m^2$), yields a value of 3.10^{-11} A cm^{-2}, which is in the range of the values determined for this family of materials [3].

The electrode impedance exhibits a simple form, resulting from the parallel combination of the double layer capacitance and the Faradaic impedance which corresponds, for the aforementioned mechanism, to the transfer charge resistance

$$Z = \frac{R_{ct}}{1 + (j\omega R_{ct} C_{dl})^{\phi}}$$

where $R_{ct} = (U_T/2.3I_0)\exp(\alpha nF\eta/RT)$ and ϕ the empirical exponent reflecting heterogeneity effects of the electrode material. The complex-plane representation of this impedance gives rise to a more or less depressed semicircle identical to that measured experimentally. Its size decreases exponentially, in accordance with the above formula, as the overpotential becomes more cathodic, but the product of the term R_{ct} times the dc current equals the constant value U_T.

3.4.2. Oxygen electrode reaction

In contrast to hydrogen evolution, there is no common concept about the mechanism of the elementary reactions that proceed during oxygen evolution on the PbO_2 electrode. According to the results of early investigations, evolution of oxygen in acid media is considered to come from discharge of water molecules to form adsorbed OH radicals. These radicals are oxidized to yield adsorbed oxygen atoms, which combine subsequently to produce oxygen molecules [14,15]. The first step is supposed to be rate determining and would then be responsible for the large capacitive loop observed at low frequencies on the impedance diagram.

The origin of the high frequency loop is not obvious. It would not be related with an electrochemical step in view of its weak sensitivity to electrode polarization (7 mV per decade). On the other hand, ascription of such a loop to relaxation of charge carriers in a thin layer occurring on top of the electrode surface, like the hydrated amorphous PbO_2/$PbO(OH)_2$ layer with mixed protonic–electronic conduction properties as reported by Pavlov and coworkers [16,17], is also questionable. Such a relaxation process is expected to happen in the hundreds of Hertz frequency range, which is five orders of magnitude larger than the highest relaxation frequency observed in the present measurements. The positive electrode behavior deserves further investigation to elucidate the relevant mechanism.

4. Conclusions

As a result of this work we have shown the following:

- Relaxation of the gassing processes in the lead-acid battery occur at frequencies ranging between 2 and 0.05 mHz, strongly justifying the exploration of the ultra-low frequency domain to observe the whole dynamic response of the system under study.
- Gassing reactions take place in the internal surface areas of the electrode pores under the experimental conditions reported.
- Hydrogen evolution on lead electrodes follows the mechanism, found with most soft metals, consisting of a rate determining charge transfer step followed by fast ion–atom recombination. The dc polarization curves and impedance parameters are in good agreement, presenting a mean Tafel slope of 130 mV per decade.
- According to the impedance results, oxygen evolution involves a mechanism that includes at least two steps of comparable kinetics for the larger float current values. In contrast to the step associated with the low frequency loop, which is sensitive to the electrode potential (Tafel slope = 67 mV per decade), the step corresponding to the

high frequency one has low sensitivity (slope = 7 mV per decade). The corresponding mechanism deserves further investigation.

Acknowledgements

One of the authors (A.H.) is grateful to the Alexander von Humboldt Foundation for making cooperation possible. The authors would like to thank S. Buller for valuable discussions.

References

[1] P. Mauracher, E. Karden, J. Power Sources 67 (1997) 69.
[2] E. Karden, S. Buller, R.W. De Doncker, J. Power Sources 85 (2000) 72.
[3] E. Gileadi, Electrode Kinetics for Chemists, Chemical Engineers, and Materials Scientists, VCH Publishers, New York, 1993.
[4] S. Trasatti, J. Electroanal. Chem. 111 (1980) 125.
[5] H. Bode, Lead-acid Batteries, Wiley, New York, 1977 (R.J. Brodd, K.V. Kordesch, Trans.).
[6] J. Newman, W. Tiedemann, J. Electrochem. Soc. 140 (1993) 1961.
[7] D. Berndt, R. Bräutigam, U. Teutsch, Temperature compensation of float voltage — the special situation of VRLA batteries, in: Proceedings of the 17th INTELEC Conference, The Hague, The Netherlands, 1995, p. 1.
[8] Bleiakkumulatoren, Herausgegeben von der Varta Batterie AG, 1986.
[9] N. Yahchouchi, Mesure de l'impédance d'un accumulateur tubulaire au plomb: application à la détermination de la capacité électrique, Doctorate Thesis, University of Paris VI, Paris, 1981.
[10] M. Keddam, Z. Stoynov, H. Takenouti, J. Appl. Electrochem. 7 (1977) 539.
[11] R. de Levie, in: R. Delahay (Ed.) Advances in Electrochemistry and Electrochemical Engineering, Vol. VI, 1967, p. 329.
[12] B.N. Kabanov, S. Jofa, Acta Physicochim. (USSR) 10 (1939) 617.
[13] A.N. Frumkin, J. Electrochem. Soc. 107 (1960) 461.
[14] J.P. Hoare, The Electrochemistry of Oxygen, Interscience, New York, 1968.
[15] A.I. Krasil'shchikov, Z. Fiz. Khim. 37 (1963) 531.
[16] D. Pavlov, I. Balkanov, J. Electrochem. Soc. 139 (1992) 1830.
[17] D. Pavlov, B. Monahov, J. Electrochem. Soc. 143 (1996) 3616.